

Improving the Performance of Projection-Based Image Registration

Matthew D. Sambora
The Air Force Institute of Technology
Dept. of Electrical and Comp. Eng.
WPAFB, OH 45433-7765
937-255-3636 x7553
matthew.sambora@us.af.mil

Richard K. Martin
The Air Force Institute of Technology
Dept. of Electrical and Comp. Eng.
WPAFB, OH 45433-7765
937-255-3636 x4625
richard.martin@afit.edu

Abstract—Projection-based image registration algorithms use the sum of the pixel values along a given axis of an image to detect spatial changes in temporally separated images. These algorithms have been shown to be computationally efficient and effective for aligning temporally separated images and for visually detecting sensor motion. Registering images via projections has also been shown as a method for overcoming registration errors caused by the presence of fixed pattern noise. This paper describes a method that exploits the statistical properties of images with significant autocorrelation to improve the performance of projection-based image registration algorithms. The algorithm is shown to operate in low SNR conditions and to significantly improve registration performance by as much as a factor of 4 in mean squared error over existing projection-based registration algorithms at a minimal computational cost.

optimally-sized filtering kernel in the absence of *a priori* knowledge of the image being registered.

Filtering images has been shown to improve the performance of correlation-based image registration [3], however, the mechanism for this has not been fully explained. For example, in [3] it is suggested that filtering improves registration performance by eliminating high frequency image content that is most likely to include the effects of aliasing.

Cain *et al.* note that in the presence of fixed pattern and temporal noise, projection-based methods can provide performance that is superior to that of 2-D cross correlations [4]. Furthermore, these projections can be formed entirely on some Charge-Coupled Devices (CCDs) [5]. For motion estimation purposes, this combination of readout speed and low computational complexity makes these algorithms especially attractive.

TABLE OF CONTENTS

1. INTRODUCTION.....	1
2. NOTATION AND PREVIOUS WORK	2
3. IMPROVED PROJECTION-BASED ALGORITHM	2
4. SELECTION OF OPTIMAL KERNEL SIZE	4
5. OBSERVING COVARIANCE IN IMAGES	5
6. EXPERIMENTAL RESULTS	6
7. CONCLUSIONS AND FUTURE WORK.....	7
8. ACKNOWLEDGEMENTS	8
REFERENCES	8
BIOGRAPHIES	8

1. INTRODUCTION

Image registration as described in this paper is the process of spatially aligning images which may have been taken by different sensors or were captured at different times. This spatial alignment may be used for multiframe image denoising as described in [1] or for estimating camera motion as described in [2]. The main contributions of this paper are a mathematical explanation for the general observation that low-pass filtering tends to improve the performance of correlation-based image registration algorithms [3] and an analytical method for determining an

The method described in this paper relies on the presence of correlations within images. Most naturally-occurring images captured by imaging systems exhibit some spatial correlation [4]. This spatial correlation, however, is not guaranteed. In particular, spatial correlation may be absent in natural images of free space and in images that are under sampled. For the purposes of this paper, we assume that our images are at least critically sampled. Practically, this restriction is not always necessary provided that resolved, sampled images in the focal plane of a given imaging system have feature sizes greater than one pixel in both dimensions.

As we will describe later in this paper, our ability to register shifts depends not only on spatial correlation but on variations in image content. Images of smooth, monochromatic surfaces are difficult to register even in the absence of noise. For applications such as image-based rigid-body motion estimation in micro UAVs, this difficulty may present challenges in some environments.

This paper is organized as follows: in section two we review relevant notation and previous work on registering images using projections. In section three we introduce the improved image registration algorithm that involves convolving the projections with a filtering kernel. In section four, we describe how the kernel size is chosen for a

¹ U.S. Government work not protected by U.S. copyright.

² IEEEAC paper 1105, Version 4, Updated 8 November 2007.

given image based on spatial correlation present in the image. In section five we provide a method for measuring spatial correlation present in the projections of an image. In section six, we provide experimental results showing the improvement in registration performance attributable to our algorithm. Finally, in section seven, we discuss conclusions from our work and describe ongoing and future work on image registration.

2. NOTATION AND PREVIOUS WORK

In this section we introduce the notation and mathematical assumptions that we will use throughout this paper. We also describe previous work on projection-based image registration which is directly related to our algorithm.

Say we have two $N \times N$ observations of an image i with additive noise q . Subscripting with $n \in \{1, 2\}$ to indicate the number of the observation, we can define our data such that

$$d_1(x, y) = i(x, y) + q_1(x, y), \quad 0 \leq x, y \leq (N-1) \quad (1)$$

$$d_2(x, y) = i(x - \alpha, y - \beta) + q_2(x, y), \quad 0 \leq x, y \leq (N-1) \quad (2)$$

where α and β are shifts of the diffraction-limited image i in the x and y directions. Furthermore, we define the additive noise to be independent and identically distributed Gaussian with zero mean and variance σ^2 .

As in [4], we can define the x and y projections of d_i as

$$d_{i,x}(y) = \sum_{x=0}^{N-1} d_i(x, y), \quad (3)$$

$$d_{i,y}(x) = \sum_{y=0}^{N-1} d_i(x, y). \quad (4)$$

We will use a windowing function described by Cain *et al.* in [4] and [5] as

$$w_f(z) = \begin{cases} 1, & |z - m_p| \leq (N/2 - \delta_s) \\ 0, & \text{else} \end{cases} \quad (5)$$

where the variable m_p is the value of z corresponding to the midpoint of a projection (i.e. the index of the centerpoint of the projection) and δ_s is the maximum allowable shift value between the frames.

Given the projection and the windowing function, Cain *et al.* then compute the 1-D cross correlations of the windowed projections of two images as

$$P_y(z) = \sum_{x=0}^{N-1} d_{1,y}(x) w_f(z+x) d_{2,y}^*(x+z) - \left(\sum_{j=0}^{N-1} d_{1,y}(j) w_f(z+j) \right) \bar{d}_{2,y}, \quad (6)$$

$$P_x(z) = \sum_{y=0}^{N-1} d_{1,x}(y) w_f(z+y) d_{2,x}^*(y+z) - \left(\sum_{j=0}^{N-1} d_{1,x}(j) w_f(z+j) \right) \bar{d}_{2,x}, \quad (7)$$

where the $\bar{d}_{i,z}$ denotes the scalar average of a given projection. The shift estimate is computed from these projections as

$$\hat{\alpha}_2 = \arg \max_z |P_y(z)|, \quad (8)$$

$$\hat{\beta}_2 = \arg \max_z |P_x(z)|. \quad (9)$$

Throughout this work, we calculate the covariances of image pixels based on their measured values in projections.

Since we want to deal only with information available in the projections, out of necessity, these measures of pixel covariances ignore some relationships that are evident in 2-D that are not evident in 1-D projections. Consequently, some of our covariances are better described as average covariances. We acknowledge this averaging using overbar notation and expressing these values as \overline{COV} as they occur.

Finally, we assume that our images are wide sense stationary allowing us to evaluate the temporal expected value of an image using a spatial average.

3. IMPROVED PROJECTION-BASED ALGORITHM

This section introduces our algorithm. When our environment is expected to yield images with significant local spatial correlation, and our imaging system is designed to provide images that are sampled sufficiently to detect this correlation, we can exploit these facts to significantly improve the performance of a projection-based shift estimator. We do this by applying a convolutional kernel to the projection in order to improve the signal-to-noise ratio (SNR). The length of this filter is dependent on both the sampling rate of the imaging sensor and on the characteristics of the environment that the sensor is expected to operate in. The rationale behind the design of this kernel is described below.

It is reasonable to assume that if we can improve the SNR of our projections, we should be able to improve the performance of a projection-based registration algorithm. We can calculate the SNR of an image projection as follows

where we use the y projection for illustrative purposes. Returning to (5) for our calculation of the projection of the image in the absence of noise we can calculate the variance of the projection as

$$\begin{aligned}
\text{VAR}(d_{i,y}(x)) &= E\left[\left(d_{i,y}(x)\right)^2\right] - \left(E[d_{i,y}(x)]\right)^2, \\
&= E\left[\left(\sum_{y=0}^{N-1} i(x, y)\right)^2\right] - \left(E\left[\sum_{y=0}^{N-1} i(x, y)\right]\right)^2, \\
&= E\left[\left(\sum_{y_1=0}^{N-1} i(x, y_1)\right)\left(\sum_{y_2=0}^{N-1} i(x, y_2)\right)\right] \\
&\quad - N^2(E[i(x, y)])^2, \\
&= \sum_{y_1=0}^{N-1} \sum_{y_2=0}^{N-1} E[(i(x, y_1))(i(x, y_2))] \\
&\quad - N^2(E[i(x, y)])^2, \\
&= NE[i^2(x, y)] \\
&\quad + N(N-1)E[(i(x, y_1))(i(x, y_2))] \\
&\quad - N^2(E[i(x, y)])^2, \quad y_1 \neq y_2, \\
&= N(\text{VAR}(i)) \\
&\quad + N(N-1)(\overline{\text{COV}(i(x, y_1), i(x, y_2))}), \\
&\quad y_1 \neq y_2. \tag{10}
\end{aligned}$$

If the noise in our image is uncorrelated, the noise in our projection will be a random variable with variance $N\sigma_{\text{noise}}^2$. It follows that we can write the SNR of the image as

$$\begin{aligned}
\text{SNR} &= \frac{N\text{VAR}(i)}{N\sigma_{\text{noise}}^2} \\
&\quad + \frac{N(N-1)\overline{\text{COV}(i(x, y_1), i(x, y_2))}}{N\sigma_{\text{noise}}^2}, \quad y_1 \neq y_2. \tag{11}
\end{aligned}$$

From (13), it is apparent that for correlated imagery, as N increases, the variance of the noise will increase linearly and the variance of the signal will increase with the square of N . This leads to the conclusion that increasing the sampling rate of an image, thereby increasing N , will lead to higher SNRs in the image projections of correlated imagery. It also suggests that by summing individual elements of a projection together, we may be able to create image projections with higher SNRs that will yield more accurate shift estimates. In fact, we find that this is indeed the case; however, we are subject to constraints that will become evident later in this paper.

A simple way to increase N is by applying a filtering kernel that will replace each value of the projection with the sum of several points on the projection. If we assume that the spatial correlation of an image is the same in both

projections, we can define a filtering kernel of length w as

$$h_w(z) = \sum_{i=0}^{w-1} \delta(z-i). \tag{12}$$

For each projection $d_{i,x}(y)$ and $d_{i,y}(x)$, we then calculate the filtered projections

$$f_{i,x}(y) = \sum_{n=0}^{N-1} d_{i,x}(n)h_w(y-n), \tag{13}$$

$$f_{i,y}(x) = \sum_{n=0}^{N-1} d_{i,y}(n)h_w(x-n). \tag{14}$$

For imagery exhibiting spatial correlation, the effect of the aforementioned filtering is to increase the SNR of the individual projections. In order to mitigate the effects of new information entering the scene, we window one of our projections using the method described in [4]. For two images, this gives us

$$f_{1,x}(y) = \sum_{n=0}^{N-1} d_{1,x}(n)h_w(y-n), \tag{15}$$

$$f_{1,y}(x) = \sum_{n=0}^{N-1} d_{1,y}(n)h_w(x-n), \tag{16}$$

$$f_{2,x}(y) = \sum_{n=0}^{N-1} d_{2,x}(n)h_w(y-n), \tag{19}$$

$$f_{2,y}(x) = \sum_{n=0}^{N-1} d_{2,y}(n)h_w(x-n). \tag{20}$$

We then use these modified projections to compute the 1-D cross correlations of the projections of two images as

$$P_y(z) = \sum_{x=0}^{N-1} (f_{1,y}(x) - \bar{f}_{1,y}) \tag{21}$$

$$(f_{2,y}(x+z) - \bar{f}_{2,y})^* w_f(x+z),$$

$$P_x(z) = \sum_{y=0}^{N-1} (f_{1,x}(y) - \bar{f}_{1,x}) \tag{22}$$

$$(f_{2,x}(y+z) - \bar{f}_{2,x})^* w_f(y+z).$$

In terms of our original data, we can write these cross correlations as

$$P_y(z) = \sum_{x=0}^{N-1} \left(\sum_{n_1=x}^{x+w-1} d_{1,y}(n_1) - Nw \langle d_{1,y}(x, y) \rangle \right) \left(\sum_{n_2=z}^{z+w-1} d_{2,y}(n_2 + z) - Nw \langle d_{2,y}(x, y) \rangle \right)^* \quad (23)$$

$$P_x(z) = \sum_{y=0}^{N-1} \left(\sum_{n_1=y}^{y+w-1} d_{1,x}(n_1) - Nw \langle d_{1,y}(x, y) \rangle \right) \left(\sum_{n_2=z}^{z+w-1} d_{2,x}(n_2 + z) - Nw \langle d_{2,y}(x, y) \rangle \right)^* \quad (24)$$

where we indicate the mean pixel value in the windowed region $\langle d_{1,y}(x, y) \rangle$. As in the unfiltered case, we compute the shift estimates from these projections as

$$\hat{\alpha}_2 = \arg \max_z |P_y(z)|, \quad (25)$$

$$\hat{\beta}_2 = \arg \max_z |P_x(z)|. \quad (26)$$

4. SELECTION OF OPTIMAL KERNEL SIZE

This section describes how we choose the size of the filtering kernel $h_w(z)$ introduced in (14). As we will show in the results section of the paper, the choice of the size of the filtering kernel is crucial to the performance of our algorithm.

Equation (13) describes the SNR of an image projection; however, predicting the performance of a correlation-based image registration algorithm requires a more involved analysis than an SNR figure can provide. If we look only at the SNR of the projections, it would appear that we could achieve increases in SNRs for as long as we are able to increase the kernel size. In practice, however, this is not the case. As described in detail in [4], the ability to detect a shift between projections of two images of the same scene depends on the amount of noise in the images and the difference between points on the cross-correlation of the projections corresponding to various shifts. As the kernel size increases, the average magnitude of points our cross-correlation increase; however, the shape of the cross-correlation becomes increasingly flat. This flattening with increasing kernel size inhibits our ability to differentiate between points on the cross correlation in the presence of noise.

Cain *et al.* in [4] describe a figure of merit (FOM) that can be used to evaluate the performance of an image registration algorithm. In this section we modify this FOM so that it can be used to evaluate the performance of our improved image registration algorithm. We then maximize the modified

FOM in an attempt to minimize the MSE of our registration errors.

Cain's FOM is defined such that z is a point on the cross correlation between two projections and α and β are the actual shifts in the x and y directions. Where the expectation indicates averaging over many frames of the identical scene, we can write



Figure 1 - 1024x1024 image of the Pentagon taken from the University of Southern California's image processing library at <http://sipi.usc.edu/database/>.

$$F_{P_y}(z, \alpha) = \frac{(E[P_y(\alpha)] - E[P_y(z)])^2}{E[\text{VAR}[P_y(z) | i] + \text{VAR}[P_y(\alpha) | i]]}, \quad (27)$$

$$F_{P_x}(z, \beta) = \frac{(E[P_x(\beta)] - E[P_x(z)])^2}{E[\text{VAR}[P_x(z) | i] + \text{VAR}[P_x(\beta) | i]]}. \quad (28)$$

While this model was shown to be effective in evaluating the performance of 2-D cross correlation and projection-based registration algorithms, we find that it is necessary to modify it for use with our algorithm. The problem lies in measuring the variance of the terms in the denominators (27) and (28). In our algorithm, applying a convolution kernel of any size other than one to the projections leads to a 1-D cross correlation function with spatially correlated noise. Since the noise is no longer i.i.d. in the points on the cross-correlation, the denominator in Cain's FOM no longer accurately reflects the vertical distance between two points on the cross-correlation.

With correlated noise in adjacent points of the cross-correlation, a measurement of the variance of the difference between these two points will be a more significant measure of noise than the sum of variances at the two points. We

therefore use the modified figures of merit:

$$F_{P_y}(z, \alpha) = \frac{(E[P_y(\alpha)] - E[P_y(z)])^2}{\text{VAR}[P_y(z) - P_y(\alpha)]}, \quad (29)$$

$$F_{P_x}(z, \beta) = \frac{(E[P_x(\beta)] - E[P_x(z)])^2}{\text{VAR}[P_x(z) - P_x(\beta)]}. \quad (30)$$

Using the assumption that our noise is i.i.d. in each pixel, it can be shown that if we filter the projections with a kernel of size w and use a windowing function of size L before we calculate their 1-D correlations, we can write for the filtered projections of an $N \times N$ image:

$$F_{P_y}(0, -1 | w, N) = \frac{(N^2 L (\text{VAR}[i(x, y_1)] - \overline{\text{COV}}[i(x, y_1), i(x+w, y_2)]))^2}{w^2 N^2 L (2(\text{VAR}[i(x, y)] - \overline{\text{COV}}[i(x, y_1), i(x+w, y_2)])\sigma^2 + \sigma^4)} \quad (31)$$

Assuming that we have an accurate model of spatial correlation in our image, we can attempt to find an optimal size for the filtering kernel for projections. With an analytic expression for F_{P_y} given by (31), we can find an optimal kernel size for a given projection of an image as

$$w_{y, \text{opt}} = \arg \max_w F_{P_y}(0, -1 | w, N). \quad (32)$$

5. OBSERVING COVARIANCE IN IMAGES

In order to perform the maximization described in (32), we need to be able to measure the average spatial covariance term $\overline{\text{COV}}[i(x, y_1), i(x+w, y_2)]$ that is used in (31). This section provides a method for measuring this average spatial covariance in noise-free images.

The covariance of two random variables is defined as $\text{COV}(X, Y) = E[XY] - E[X]E[Y]$ [6]. Because measuring the covariance present in an image is required to compute and maximize the FOM, we take time to describe the measurement of covariances in intensity images and their projections. We also examine the effect of additive noise on these covariances.

For a given image, we need to be able to determine the covariance terms that affect our ability to register the image using projections. Here we describe a simple way of determining these parameters using fast calculations that employ simple image parameters. Say we have a projection of an image d_i , such that

$$\begin{aligned} d_{1,y}(x) &= \sum_{y=0}^{N-1} d_1(x, y), \\ &= \sum_{y=0}^{N-1} [i(x, y) + q_1(x, y)], \\ &= \sum_{y=0}^{N-1} i(x, y) + \sum_{y=0}^{N-1} q_1(x, y). \end{aligned} \quad (33)$$

In this equation we can define

$$I_y(x) = \sum_{y=0}^{N-1} i(x, y), \quad (34)$$

so that $I_y(x)$ is the projection of a diffraction limited image taken along the x axis. We then note that:

$$\begin{aligned} E[I_y^2] &= E\left[\left(\sum_{y=0}^{N-1} i(x, y)\right)^2\right], \\ &= E\left[\left(\sum_{y_1=0}^{N-1} i(x, y_1)\right)\left(\sum_{y_2=0}^{N-1} i(x, y_2)\right)\right], \\ &= \sum_{y_1=0}^{N-1} \sum_{y_2=0}^{N-1} E[(i(x, y_1))(i(x, y_2))], \\ &= NE[i^2(x, y)] \\ &\quad + N(N-1)E[i(x, y_1)i(x, y_2)], \quad y_1 \neq y_2. \end{aligned} \quad (35)$$

We then note that the variance of the projection can be calculated as

$$\begin{aligned} \text{VAR}[I_y] &= E[I_y^2] - E[I_y]^2, \\ &= NE[i^2(x, y)] \\ &\quad + N(N-1)E[i(x, y_1)i(x, y_2)] \\ &\quad - N^2 E[i(x, y)]^2, \quad y_1 \neq y_2 \\ &= N\text{VAR}[i(x, y)] \\ &\quad + N(N-1)\overline{\text{COV}}[i(x, y_1), i(x, y_2)], \quad y_1 \neq y_2. \end{aligned} \quad (36)$$

This shows us that we can easily calculate the covariance of a projection in the image from the measured values of the variance of the pixel intensities in an image and the variance of the projection. Specifically,

$$\begin{aligned} \text{COV}[i(x, y_1), i(x, y_2)] \\ &= \frac{\text{VAR}[I_y] - N\text{VAR}[i(x, y)]}{N(N-1)}, \quad y_1 \neq y_2. \end{aligned} \quad (37)$$

We will find it convenient to remove the restriction

$y_1 \neq y_2$ and calculate the covariance as

$$\begin{aligned}
E[I_y^2] &= E\left[\left(\sum_{y=0}^{N-1} i(x, y)\right)^2\right], \\
&= E\left[\left(\sum_{y_1=0}^{N-1} i(x, y_1)\right)\left(\sum_{y_2=0}^{N-1} i(x, y_2)\right)\right], \\
&= \sum_{y_1=0}^{N-1} \sum_{y_2=0}^{N-1} E[i(x, y_1)i(x, y_2)], \\
&= N^2 E[i(x, y_1)i(x, y_2)] \\
&\quad - N^2 E[i(x, y)]^2 + N^2 E[i(x, y)]^2, \\
&= N^2 \overline{\text{COV}}(i(x, y_1), i(x, y_2)) + N^2 E[i(x, y)]^2. \quad (38)
\end{aligned}$$

So, for a given projection, we can easily calculate a measured covariance as

$$\begin{aligned}
&\overline{\text{COV}}(i(x, y_1), i(x, y_2)) \\
&= \frac{1}{N^2} (E[I_y^2] - N^2 E[i(x, y)]^2). \quad (39)
\end{aligned}$$

If we want to measure the covariance between the projection of an image and the image at an arbitrary shifted value z , we can substitute $I_y(x+z)$ into the calculation above and arrive at the expression

$$\begin{aligned}
&\overline{\text{COV}}(i(x, y_1), i(x+z, y_2)) \\
&= \frac{1}{N^2} (E[I_y(x)I_y(x+z)] - N^2 E[i(x, y)]^2). \quad (40)
\end{aligned}$$

These calculations are, of course, identical for projections along the rows and columns of the images. The measured covariance of an image in two dimensions can be defined as

$$\begin{aligned}
&\overline{\text{COV}}(i(x, y), i(x+\alpha, y+\beta)) \\
&= E[i(x, y), i(x+\alpha, y+\beta)] - E[i(x, y)]^2. \quad (41)
\end{aligned}$$

Sample plots of covariances measured by circularly shifting the horizontal and vertical projections of an image are shown in Figs 1-3.

Although these covariance calculations are performed using noise-free images this method can be modified for use with noisy images. In the presence of uncorrelated noise, the correlation properties of the image are unchanged and estimates of the curves shown in Figs. 3 and 4 can be estimated from available data.

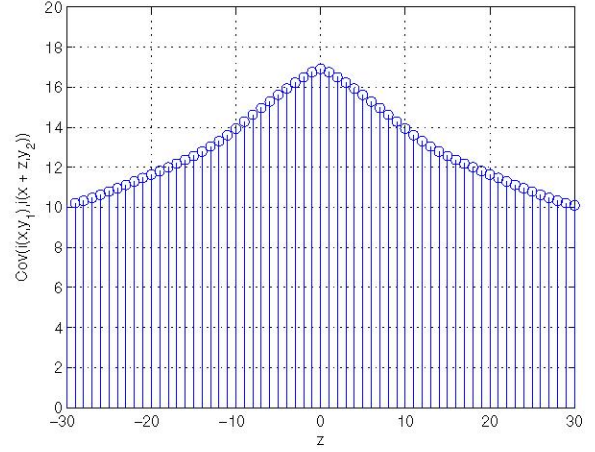


Figure 2 - Measured covariance of the horizontal projection of the image shown in Fig. 1.

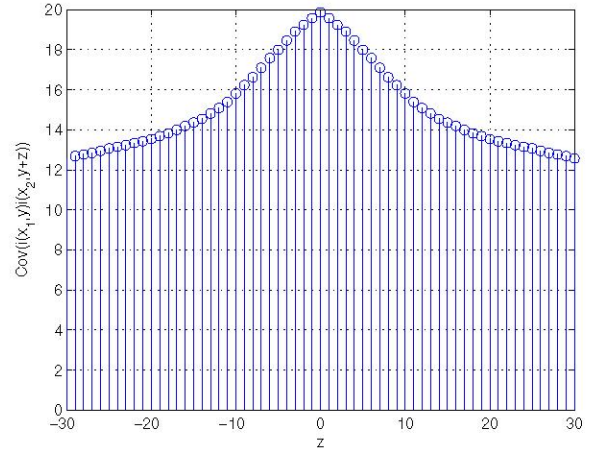


Figure 3 - Measured covariance of the vertical projection of the image shown in Fig. 1.

6. EXPERIMENTAL RESULTS

In this section we describe experimental results produced by our algorithm.

The algorithm was tested on the 1024×1024 Pentagon image shown in Fig. 1 by adding AWGN to two frames with $\sigma=100$. We measured the accuracy of our registration algorithm by estimating shifts for two frames when the actual shift was zero. We used an estimate of the correlation function for the window which was calculated by circularly shifting a windowed, noise-free projection of our image. In an actual imaging system, we could assume an expected correlation model or could estimate the correlation model from the noisy data.

For kernel sizes from 1 to 30 we produced 1000 pairs of frames (i.e. a total of 30,000 trials) and estimated the shift from the projections of the two images. Without filtering the projections, we achieved a MSE of 1.41. After filtering, we were able to improve our estimates significantly. Our algorithm estimated a peak F_{py} when the kernel size was 11 and which produced a measured MSE of 0.38. The highest measured peak of F_{py} occurred with a kernel size of 8 and yielded an MSE of 0.38 as well. Our lowest measured MSE was with a kernel size of 7 and a MSE of 0.36. These results are displayed graphically in Fig. 4 and 5.

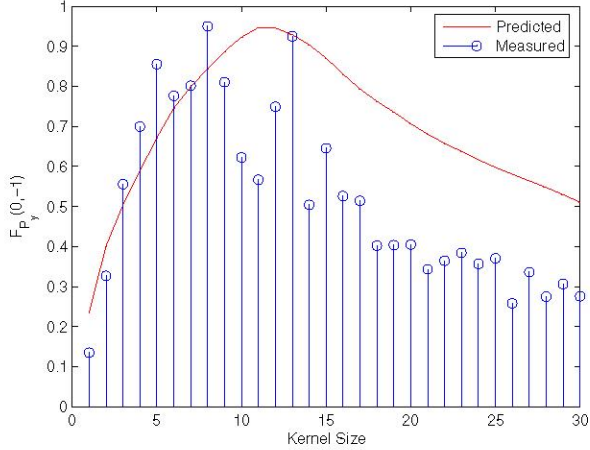


Figure 4 - Predicted vs. measured results for figure of merit calculations over 100 noise realizations and various kernel sizes. Measured results are shown as stem points. Predicted results are shown as a line plot. Differences at large kernel sizes are attributable to local biases.

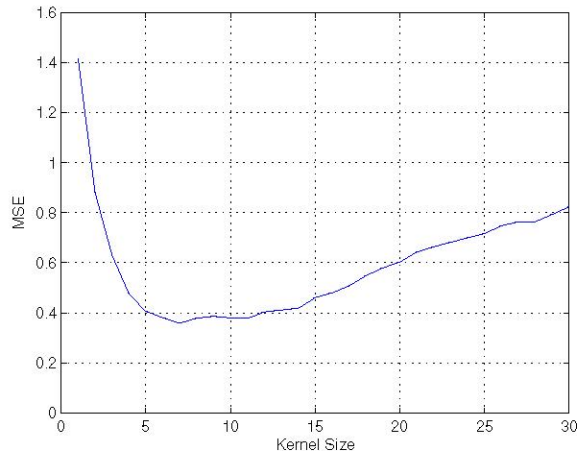


Figure 5 - Measured mean squared error of shift estimates for an actual shift of zero and additive noise with $\sigma = 100$.

Two main sources of error were evident in our experiments. A primary source of error was local image bias. A model

of spatial correlation developed using circular shifting of a windowed image incurs bias at shifts other than zero. The effect of bias is evident in Figure 4 where the predicted F_{py} begins to deviate from the measured F_{py} as the kernel size increases above approximately 8. A second source of error between kernel size and lowest MSE was the way we calculated the expected shift. Our algorithm is designed to minimize errors occurring between shifts of 0 and -1 which was the shift most likely to produce an error. However, statistically, we can expect errors produced by other shifts that will contribute to our MSE. A more complete model could account for these additional shifts.

7. CONCLUSIONS AND FUTURE WORK

This paper has provided a method for improving the performance of projection-based image registration algorithms. It also provides a mathematical explanation for the general observation that low-pass filtering tends to improve the performance of image registration algorithms and that hierarchical separation of frequency content can be used for motion estimation [3], [7]. In the preceding sections, we have described an algorithm that improves the performance of current projection-based image registration and have described methods for choosing optimal parameters for the algorithm based on measured data from the images being registered.

One possible extension to this work would be an algorithm that had a more direct link between kernel size, shape, and MSE. As mentioned earlier in this paper, our algorithm is designed to minimize errors in registration between $z = 0$ and $z = -1$ (i.e. the shift most likely to produce an error.) A more complete model might include the error contributions of other shifts and estimate the kernel size and shape expected to minimize MSE over all shifts.

As with most image registration algorithms [2], we also note that our results are affected, sometimes severely, by local biases in images. These effects are most pronounced in smaller images that are highly windowed. For these types of image conditions, we expect that this algorithm will be most effective when our image content is periodic. Large image sizes with small expected shifts (and thus, less windowing) also provide favorable conditions for algorithm employment. Future work may include an exploration of methods for mitigating the effects of bias in the estimator.

Transform-domain operations provide a mechanism for registering images that are not only translated but also dilated or rotated. Use of the filtering method described in this paper with dilated or rotated images is another possible extension to this research.

The correlation theory contained in this paper may also be applied to a host of other applications. An obvious extension to the work contained in this paper is studying the effect that filtering has on two-dimensional correlation

problems.

communications, terrestrial telecommunications and networking, contracting and enterprise computing.

8. ACKNOWLEDGEMENTS

The opinions and views expressed by the authors are not necessarily those of the Department of Defense or the United States Air Force. This document has been approved for public release; distribution unlimited.

REFERENCES

- [1] A. MacDonald, "Blind Deconvolution of Anisoplanatic Images Collected by a Partially Coherent Imaging System," Ph.D. dissertation, Air Force Institute of Technology, Wright-Patterson AFB, OH, June 2006.
- [2] D. Robinson and P. Milanfar, "Fundamental Performance Limits in Image Registration," *IEEE Transactions on Image Processing*, vol.13, no.9, pp. 1185--1189, Sept 2004.
- [3] J. R. Bergen, P. Anandan, K.J. Hanna, and R. Hingorani, "Hierarchical Model-Based Motion Estimation." In *Proceedings of the Second European Conference on Computer Vision (May 19 - 22, 1992)*. Springer-Verlag, London, pp. 237--252. 1992.
- [4] S. C. Cain, M. M. Hayat and E. E. Armstrong, "Projection-Based Image Registration in the Presence of Fixed-Pattern Noise," *IEEE Transactions on Image Processing*, vol. 28, no. 12. pp. 1860--1870, 2001.
- [5] S. C. Cain, "Design of an Image Projection Correlating Wavefront Sensor for Adaptive Optics," *Optical Engineering*, vol. 43, pp. 1670--1681, July 2004.
- [6] A. L. Garcia, *Probability and Random Processes for Electrical Engineers*. 2nd ed., Reading, MA: Addison Wesley Longman, 1994.
- [7] P. J. Burt and E. H. Adelson, "The Laplacian Pyramid as Compact Image Code," *IEEE Transactions on Communications*, vol. 31, no. 4, pp. 532--540, April 1983.

BIOGRAPHIES

Lt Col Matthew D. Sambora is a 19-year veteran of the United States Air Force and is currently a doctoral student at the Air Force Institute of Technology (AFIT). Lt Col Sambora earned a BS degree in Electrical and Computer Engineering from Clarkson University in 1988 and an MS from Southern Illinois University at Edwardsville in 1996. His assignments have been in both leadership and technical areas and have encompassed heavy construction, satellite



Dr. Rick Martin is an Assistant Professor at the Air Force Institute of Technology (AFIT) in Dayton, Ohio, where he is the signal processing curriculum chair and the graduate electrical engineering program chair. AFIT Students have voted him "Instructor of the Quarter" (three times) for the ECE Department and Eta Kappa Nu instructor of the year. His research interests include equalization for multicarrier communication systems; blind, adaptive algorithms; sparse adaptive filters; cognitive radio; and image registration. He has authored thirteen journal papers, twenty-three conference papers, a book chapter, and four patents.